Mem. S.A.It. Suppl. Vol. 24, 100

Memorie della
Supplementi

First steps with CO5BOLD using HLLMHD and PP reconstruction

O. Steiner[1], S. P. Rajaguru[2], G. Vigeesh[3], M. Steffen[4], W. Schaffenberger[5], and B. Freytag[6]

[1] Kiepenheuer-Institut für Sonnenphysik, Schöneckstrasse 6, 79104 Freiburg, Germany
e-mail: steiner@kis.uni-freiburg.de
[2] Indian Institute of Astrophysics, Koramangala II Block, Bangalore 560 034, India
[3] Dep. of Astronomy, New Mexico State University, Las Cruces, NM 88003-8001, USA
[4] Leibniz-Institut für Astrophysik (AIP), An der Sternwarte 16, 14482 Potsdam, Germany
[5] Bahnhofstraße 1, 9560 Feldkirchen, Austria
[6] Centre de Recherche Astrophysique de Lyon, UMR 5574, CNRS, Université de Lyon, École Normale Supérieur de Lyon, 46 allée d'Italie, 69364 Lyon Cedex 07, France

Abstract. We report on first experiences with real-life applications using the MHD-module of CO5BOLD together with the piecewise parabolic reconstruction scheme and present preliminary results of stellar magnetic models with $T_{\rm eff}$ = 4000 K to $T_{\rm eff}$ = 5770 K.

Key words. Magnetohydrodynamics (MHD) – Methods: numerical – Convection – Stars: atmospheres – Stars: activity – Stars: magnetic fields

1. Introduction

CO5BOLD is a radiation-hydrodynamics code for the numerical simulation of stellar surface layers in three spatial dimensions.It is also used for the simulation of entire stars. The code and applications of it are described in Freytag et al. (2012). Two different approximate Riemann solvers are used—a Roe type solver (Roe 1986) for the integration of the hydrodynamical equations, and an extension of the HLL solver (Harten et al. 1983) for the integration of the magnetohydrodynamical equations. Each of these solvers can be combined with different methods for the reconstruction of a piecewise continuous solution from the numerical solution given at discrete nodes (Freytag 2013). Piecewise linear reconstruction is used with the van Leer scheme, while PP uses a piecewise parabolic reconstruction (Colella & Woodward 1984). The reconstructions yield left and right states at computational cell interfaces, which defines the Riemann problem to be resolved with the Riemann solver (see, e.g., Toro 2009).

In the past, numerous applications with CO5BOLD have been carried out using HLLMHD in combination with the van Leer reconstruction scheme (e.g., Schaffenberger et al. 2006; Steiner et al. 2008, 2010; Kato et al. 2011; Nutto et al. 2012; Steiner & Rezaei 2012; Wedemeyer-Böhm et al. 2012). Here, we report on first experiences obtained with HLLMHD in combination with the PP reconstruction scheme, using the code version 002.00.2011.04.28. While standard 1-D and

Send offprint requests to: O. Steiner

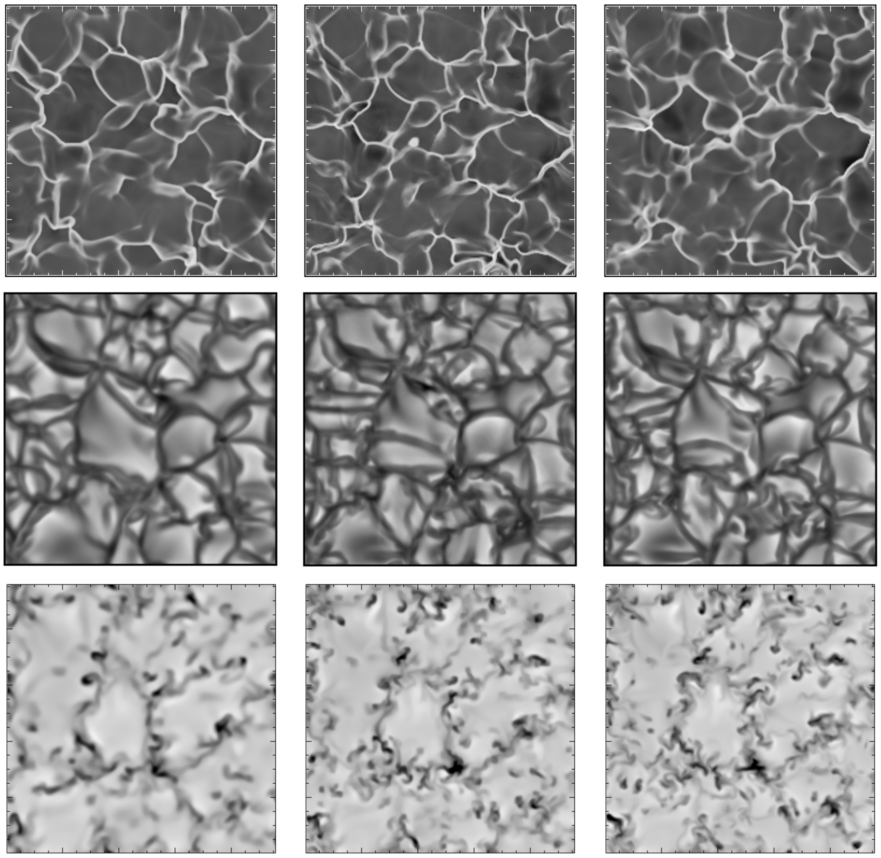

Fig. 1. Temperature in a horizontal section 1200 km above the solar surface of $\tau_5 = 1$ *(top row)*, bolometric intensity *(middle row)*, and vertical velocity at 800 km depth (bottom row) of a magnetic field free simulations in a box of side lengths 9.6 Mm. The grid constant in the horizontal directions is 40 km. Starting from a unique model, it was advanced for 540 s with different combinations of Riemann solvers and reconstruction methods. *Left:* HLLMHD and van Leer; *Middle:* HLLMHD and PP; *Right:* Roe and van Leer.

multi-dimensional test problems were carried out in the course of the code development, we give in Sect. 2 a qualitative comparison between different schemes when applied to real-life problems and discuss applications to stellar atmospheres in Sect. 3.

2. Qualitative comparisons

The PP reconstruction is formally of higher order accuracy than the van Leer reconstruction. On the other hand, the Roe solver is more accurate than the HLL solver because it approximates the true Riemann solution in more details than HLL does. It is therefore interesting to ask whether the HLLMHD solver in combination with PP performs as well as the standard hydrodynamic module of CO5BOLD, which combines the Roe solver with the van Leer reconstruction scheme (but see Freytag 2013, for the latest standard combination for hydrodynamics). Of course, we can answer this question only for a magnetic field free model atmosphere because the implemented standard Roe solver works without magnetic field only. On the other hand, HLLMHD also works when setting the magnetic field to zero.

The middle row of Fig. 1 shows the emergent bolometric intensity from the surface of a solar model with a field of view of 9.6×9.6 Mm^2. Starting from a unique model, it was advanced for 540 s, which is of the order of the granulation life-time. We see that the HLLMHD solver in combination with the van Leer reconstruction scheme (left panel) produces a distinctly more diffusive solution than the HLLMHD solver in combination with the piecewise parabolic reconstruction PP (middle panel). The latter combination produces much more granular substructure than HLLMHD with van Leer does. At the same time it produces a solution, which is much closer to the solution obtained with the Roe solver in combination with van Leer (right panel), which was the standard combination for pure hydrodynamic simulations in the past.

The same statement can be made regarding the temperature structure at a height of 1200 km above $\tau_5 = 1$, which is shown in the top row of Fig. 1. This height level corresponds to the lower chromosphere. There, magnetic field free simulations produce a distinct meshwork of shock fronts (Wedemeyer et al. 2004). Despite the fact that the time scale of this shock meshwork is much shorter than the granulation life-time, the solution produced by HLLMHD in combination with PP its quite similar to the standard combination Roe plus van Leer.

The bottom row shows the vertical velocity between -10 km s^{-1} (downflow, black) and $+4$ km s^{-1} (upflow, white) in a depth of 800 km below $\tau_5 = 1$. Once again, HLLMHD with the van Leer reconstruction is distinctly more diffusive than the other two schemes. At this depth level, however, HLLMHD with PP does not really match the solution produced by the Roe solver very well. Details differ, in particular, shapes and strengths of down flow plumes. On the other hand, the solution produced by HLLMHD and PP reconstruction looks barely more diffusive than that obtained with the Roe solver.

When introducing magnetic fields, HLLMHD with PP produces wiggles and saw-teeth in the internal energy and derived quantities (especially the temperature) at chromospheric heights (see Fig. 2 as an example).

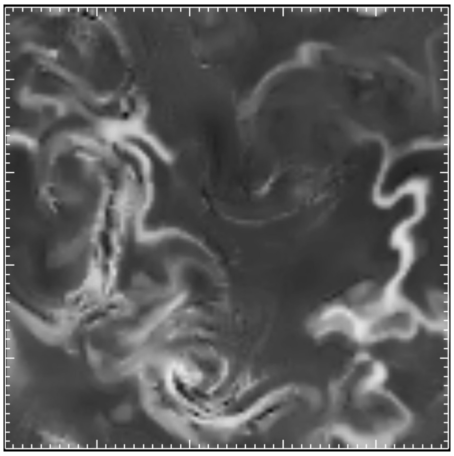

Fig. 2. Temperature in a horizontal section 1200 km above the solar surface of $\tau_5 = 1$ of a model with an initially homogeneous, vertical magnetic field of strength 50 G and a box side-lengths 4.8 Mm. HLLMHD and PP was used to advance the solution. While showing much more details than HLLMHD plus van Leer, it also produces wiggles, saw-teeth, and single cells with very low temperature.

Here, PP seems to act too aggressive (see also Freytag 2013, in this volume). Interestingly, this problem occurs with magnetic field only and disappears when setting $\boldsymbol{B} = 0$.

At first, we experienced with HLLMHD plus PP strong overstable oscillations of the entire atmosphere when computing models with effective temperature $T_{\rm eff} = 5000$ K and even more so with $T_{\rm eff} = 4000$ K. We traced this problem back to the employed time integration scheme: when the original Hancock time-integration scheme was replaced by the second order Runge-Kutta scheme, the problem disappeared. Meanwhile, a more consistent (higher temporal order) treatment of the gravitational terms with the Hancock scheme, yet to be tested, should have remedied this problem (B. Freytag, W. Schaffenberger, priv. comm.).

3. The magnetic fine structure of stellar atmospheres

Other than the solar atmosphere with $T_{\rm eff} = 5770$ K, we have also computed stellar models with $T_{\rm eff} = 5000$ K and $T_{\rm eff} = 4000$ K.

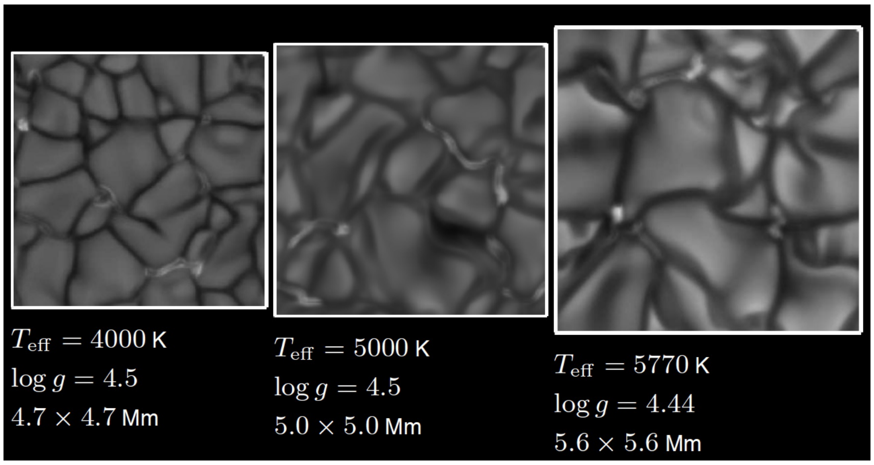

Fig. 3. Emergent bolometric intensity of models with effective temperature, surface gravity, and field-of-view as indicated. The initial models were supplemented with a homogeneous, vertical magnetic field of 50 G and advanced for 1 to 3 hours using HLLMHD with PP reconstruction.

Example snapshots of these simulations are shown in Fig. 3. Since the average size of granules approximately scales with the pressure scale-height, it decreases with decreasing effective temperature, as does the contrast (Freytag et al. 2012). All the time instants of Fig. 3 show a bright filigree in the form of sheets, dots, and crinkles, which coincide with locations of magnetic flux concentrations. They look similar in all three snapshots, maybe with the tendency of being more roundish and crinkle-like at $T_{\rm eff}$ = 4000 K and more sheet like for the solar model. At this point, we have not yet verified whether the appearance of double layered sheets are a consequence of physically real 'hot walls' or if they are rather an artifact of the PP reconstruction being too aggressive

Table 1 lists a few properties of the strongest small-scale magnetic flux concentrations that evolve in the three models of Fig 3. The second column lists the mean (from n snapshots) of the maximal field strength at optical depth unity. The third column is the corresponding mean of the maximal field strength at the fixed geometrical height where the mean optical depth is unity. The geometrical difference between these two depth levels (again averaged over n snapshots) is termed WD, in reminiscence of the Wilson depression. $B_{\rm eq\,th}$ is computed from the mean gas pressure at mean optical depth unity from $B_{\rm eq\,th} = \sqrt{8\pi p_{\rm gas}(\langle\tau\rangle = 1)}$. These are results of a very preliminary analysis with only a few snapshots taken into account, analyzed 'by hand', i.e., not in a systematic and very accurate manner.

We note the following: (1) $B_{\rm max}(\tau = 1)$ stays fairly constant, (2) $B_{\rm max}(\langle\tau\rangle = 1)$ steeply increases with decreasing temperature, (3) the Wilson depression drops more rapidly with decreasing effective temperature than one would expect from the drop in the pressure scale-height, and (4) while $B_{\rm max}(\langle\tau\rangle = 1)$ assumes super equipartition values for the solar model, it does clearly not so for the model with $T_{\rm eff}$ = 4000 K. Property (3) can be seen to be a consequence of property (4), which itself is possibly a consequence of the reduction of convective velocities with decreasing temperature. Given property (1), property (2) can be understood in terms of property (3) but essentially, it is due to the fact that the optical depth unity drops to deeper layers of higher pressures and densities with decreasing temperature. Most intriguing is property (1).

An interesting open question is the radiative energy budget of magnetic vs. nonmagnetic stellar models because it relates to

Table 1. Properties of small scale magnetic flux concentrations of three model atmospheres with different effective temperatures, $T_{\rm eff}$. Field strengths are given in G. τ is a Rosseland mean optical depth, WD the Wilson depression in km, $B_{\rm eq\,th}$ the approximate thermal equipartition field strength at the fixed geometrical height of mean optical depth $\langle\tau\rangle = 1$, and H_p the approximate pressure scale-height in km. n is the number of snapshots that were analyzed. The indices give the extreme deviations from the given value found in n snapshots.

$T_{\rm eff}$	$B_{\rm max}(\tau = 1)$	$B_{\rm max}(\langle\tau\rangle = 1)$	WD	$B_{\rm eq\,th}$	H_p	n
5770	2567^{+310}_{-252}	1616^{+168}_{-81}	315^{+45}_{-28}	1497	142	6
5000	2619^{+471}_{-339}	1876^{+108}_{-130}	154^{+45}_{-29}	1884	118	10
4000	2593^{+451}_{-236}	2056^{+91}_{-90}	73^{+16}_{-14}	2571	84	9

the photometric variability of a star in function of its magnetic cycle. Since the outwardly directed radiative flux at the top of the computational domain is considerably fluctuating in time for a finitely sized box, one would have to run extremely long time series for accurately determining differences between the magnetic and the non-magnetic model.

Here, we propose a straightforward solution to this problem, which consists in constructing a magnetic mask. The unmasked area, A_0 (with field strength below a certain level) defines the 'quiet star' region with the mean bolometric intensity I_0. The masked area, $A_{\rm mag}$, defines the mean intensity of the magnetic features, $I_{\rm mag}$. Here, "mean" means spatial average over the respective mask. Thus,

$$\delta = \frac{\langle A_0 I_0 + A_{\rm mag} I_{\rm mag}\rangle - \langle (A_0 + A_{\rm mag}) I_0\rangle}{\langle (A_0 + A_{\rm mag}) I_0\rangle}$$

defines the relative radiative surplus or deficit of the magnetic model with respect to a hypothetically field-free model. The average $\langle ...\rangle$ is taken over a suitable time period. However, caution is indicated because this approach implicitly assumes that the unmasked area is not influenced by the magnetic field at all, viz., that $\langle I_0\rangle$ is the mean intensity of a model without magnetic field.

References

Colella, P. & Woodward, P. R. 1984, J. Comput. Phys., 54, 174

Freytag, B. 2013, Mem. Soc. Ast. Italiana, this volume

Freytag, B., Steffen, M., Ludwig, H.-G., et al. 2012, J. Comput. Phys., 231, 919

Harten, A., Lax, P. D., & van Leer, B. 1983, SIAM Review, 25, 35

Kato, Y., Steiner, O., Steffen, M., & Suematsu, Y. 2011, ApJ, 730, L24

Nutto, C., Steiner, O., Schaffenberger, W., & Roth, M. 2012, A&A, 538, A79

Roe, P. L. 1986, Ann. Rev. Fluid Mech., 18, 337

Schaffenberger, W., Wedemeyer-Böhm, S., Steiner, O., & Freytag, B. 2006, in ASP Conf. Ser., Vol. 354, Solar MHD Theory and Observations, ed. J. Leibacher, R. F. Stein, & H. Uitenbroek, 345–350

Steiner, O., Franz, M., Bello González, N., et al. 2010, ApJ, 723, L180

Steiner, O. & Rezaei, R. 2012, in ASP Conf. Ser., Vol. 456, Fifth Hinode Science Meeting, ed. L. Golub, I. De Moortel, & T. Shimizu, 3–32

Steiner, O., Rezaei, R., Schaffenberger, W., & Wedemeyer-Böhm, S. 2008, ApJ, 680, L85

Toro, E. F. 2009, Riemann Solvers and Numerical Methods for Fluid Dynamics, 3rd edn. (Springer)

Wedemeyer, S., Freytag, B., Steffen, M., Ludwig, H.-G., & Holweger, H. 2004, A&A, 414, 1121

Wedemeyer-Böhm, S., Scullion, E., Steiner, O., et al. 2012, Nature, 486, 505